

## Natural Radioactivity in Wadi Muhrim, Taif, Saudi Arabia

Dheya Al-Othmany

Nuclear Engineering Department, College of Engineering,  
King Abdulaziz University, Jeddah, Saudi Arabia

P. O. Box 80029, Jeddah, 21589

Email: [dothmany@kau.edu.sa](mailto:dothmany@kau.edu.sa)

### ABSTRACT:

During the past decades, the population in Saudi Arabia expanded significantly causing an increase in demand of land for housing. Some people, such as people in Wadi Muhrim area in the Taif region, decided to build their homes near the mountains and in the valleys. Some of these places contain a very high level of natural radioactivity in soil and rocks. This radioactivity originates naturally from  $^{235}\text{U}$ ,  $^{238}\text{U}$  and  $^{232}\text{Th}$  series, natural  $^{40}\text{K}$ , gas  $^{222}\text{Rn}$  and its radioactive progeny; while cosmic rays mostly come from the Galaxy's and extragalactic disk. Recent investigations have been carried out in the area to follow-up and to conduct case-control studies for these radio-ecological elements. The author investigated and developed radiological maps for soil, water and air in the area to record the highest radiation level locations. Investigations included assessment of doses on the public health to create rules and regulations concerning habitat, agriculture products and utilization of building materials from these areas. The main purpose of this study is to keep data records and radiological maps of the area in order to ascertain possible changes in the environmental radioactivity due to nuclear, industrial, and other human activities.

### INTRODUCTION

During the past decades, the population in Saudi Arabia expanded significantly causing an increase in demand of land for housing. Some people, such as people in Wadi Muhrim area in Taif region, decided to build their homes near the mountains and in the valleys. Some of these places contain a very high level of natural radioactivity from rocks & soil. Soil is the upper part of the earth's crust and consists of minerals, organic matter, water & air. The percentages of these materials vary widely according to soil type, usage, and particle size [1]. Environmental sources can be divided into:

1) *Natural radiation* depends on location, altitude and geochemical effects that cause enhanced levels of terrestrial radiation. It is never absent and has been irradiating all forms of life since the beginning of creation. Great interest in the study of NORM external and internal hazards to human beings have been noticed during the exploration of uranium and uranium bearing rocks [2-6].  $^{235}\text{U}$ ,  $^{238}\text{U}$  and  $^{232}\text{Th}$  series and natural  $^{40}\text{K}$  occur at trace levels in ground formations as a consequence of radioactive decay and depend upon the local geology and geography of the region. Table 1 summarizes the activity concentration of these materials in soil samples worldwide [7]. In addition to the table,  $^{222}\text{Rn}$  gas and its radioactive progeny, which has a half-life of 3.8 days with decay product of radium-226 and ultimately of uranium-238. Radon can accumulate in enclosed areas such as underground mines and houses. When inhaled into the lungs, alpha particles emitted by short-lived decay products of radon can damage cellular DNA. In addition, other organs, including the kidney, the stomach and the bone marrow, may receive  $^{222}\text{Rn}$  doses [8 -11].

2) *Cosmic radiation*: Some areas have high dose rates due to cosmic rays from the Galaxy's disk and extragalactic probably being the highest-energy ones. It depends on altitudes and latitudes. The details of the cosmic ray ion production, interaction and effects are discussed in detail in [12].

### Man-made Radionuclides:

The man-made (artificially produced) radionuclides can be introduced into the environment due to the proliferation of the different nuclear applications. These radionuclides have contributed to the increase in levels of environmental radioactivity. Prediction of the impacts to man and his environment is needed for each area [13-14]. Sources of man-made radionuclides include nuclear tests, nuclear power plants, reprocessing facilities, medical, industrial and agricultural applications, and those used for research purposes [15-16]. Generally, some of the non-nuclear industrial processes supply a considerable contribution to the radio-ecological pollution such as phosphate ore mining and phosphate fertilizer manufacturing and agricultural applications [15 and 17].

In terms of population radiation dose, the sources of natural radiation are the most significant and the main contributor to the population collective doses [11 and 15]. It is necessary to study this radioactivity in soil to i) assess the absorbed dose rate to the population; ii) know the health risks and iii) have a baseline for future changes in the environmental radioactivity due to human activities. Excess radiation levels can cause somatic (those affecting the body) and genetic effects (those affecting future generations). The quantitative estimation of such health risks, based on information about exposure and dose-response relationships, is fundamental to policy decisions about which risks are unacceptable and how best to manage them [18 &19].

Measurements of the radioactive properties of naturally occurring elements with instruments such as Geiger counters, scintillation meters, electrometers, and spectrometers indicate that a low level of radioactivity is present in almost all rocks and minerals. It is dependent upon the concentration of radioactive elements initially present and the change that the rock has undergone. In measuring radioactivity accurately, there are more variables than any other geophysical technique such as Atmosphere Conditions, Data Reduction and Compilation, etc [20].

In this work, we directed our efforts to 1] assess of dose rates and risk impact of the concentration of natural radioactivity for  $^{238}\text{U}$ ,  $^{226}\text{Ra}$ ,  $^{232}\text{Th}$ ,  $^{222}\text{Rn}$ ,  $^{228}\text{Ra}$  and  $^{40}\text{K}$  and cosmic ray to create rules and regulations concerning habitat, agriculture products and building materials from these areas, 2] keep data records and radiological maps of the area, in order to ascertain possible changes in the environmental radioactivity in future.

## **MATERIALS AND METHODS**

This part will deal with different practical and experimental aspects such as the description of the area of study, soil and water sampling, sample preparation, radon in water measurements, terrestrial elements like  $^{238}\text{U}$ ,  $^{232}\text{Th}$ ,  $^{40}\text{K}$ , cosmic-rays and total count field measurements, radon indoor measurements, experimental setup, calibration and theoretical calculation of radiation doses.

### **Part (1): Mapping**

#### ***1) Overview of geology of Saudi Arabia:***

The rocks of Saudi Arabia range in age from the Precambrian to the present day. This forms part of a larger unit that includes the Arabian Peninsula and is known as the Arabian Plate. Some Precambrian rocks in this region date back to the Archean (nearly 3 million years ago), but most are Neoproterozoic (1000-540 Ma\*). They originated as volcanic islands or as chains of volcanoes along spreading centers and subduction zones in a Neoproterozoic ocean and against ancient continental margins, and were folded and uplifted toward the end of the Precambrian as a large belt of mountains. The mountains existed between about 680-540 Ma and were part of one of the largest mountain belts ever known to have existed on Earth. By the end of the Precambrian, the mountains had been eroded and only their roots are preserved.

The western region of Saudi Arabia exists on the Arabian shield. The main geological divisions of Saudi Arabia are shown in Figure 1.

#### ***2) Geology of Wadi Muhrim Region:***

The Wadi Muhrim region exists in Taif on the Arabian shield in a thrust fault as shown in Figure 2. The Wadi Muhrim contains alluvium–sand and gravel surrounded by schist, meta-volcanic rocks, schistose gray wacke and some quartzo feldspathic schist. This region has a lot of subsurface water and a lot of water wells. The study region area is 25 km<sup>2</sup> and it is located at 1845m above sea level.

### **Part (2): Sampling and Preparation**

#### ***1) For Laboratory Investigations:***

**Soil Samples:** Soil samples were collected from one location in the area of the study. The samples were collected by normal methods used typically in the mountains in the area. The samples were mechanically crushed, and sieved through a 2 mm mesh sieve.

**For gamma-ray spectrometry,** an aliquot of the samples was transferred to a 300 cc capacity plastic container and sealed for about four weeks to reach secular equilibrium for measurement on a HPGe detector.

**Water Samples:** A water sample was collected from the outlet of one deep underground well. The sample was collected in 5 L capacity polyethylene container. It was transferred to the Saudi geological survey laboratory and kept in a dark cool place for preservation.

- **For Inductively Coupled Plasma- Mass Spectrometry (ICP-MS) analysis,** an aliquot of the sample, about 40 mL, was sent to a chemical laboratory at the Saudi geological survey to determine the total and leachable concentrations of U, Th and K analysis.
- **For physical and chemical property analysis,** another aliquot of the sample, about 500 mL, was sent to the water analysis lab at the Saudi geological survey. The pH, electric conductivity (EC), CaCO<sub>3</sub> percentage, soluble cations (Ca, Mg, Na, k) in mg/L and soluble anions (CO<sub>3</sub>, HCO<sub>3</sub>, Cl, SO<sub>4</sub>) in mg/L were determined by applying the standard procedures according to ICARDA organization [21].
- **For radon in water analysis,** another aliquot of the sample (approximately 500 mL) was collected in a special glass container and taken directly for measurement of radon in pCi/L using RAD7 Electronic Radon Monitor/Sniffer instrument..

## **2) For Measurement of Indoor Radon:**

Indoor radon must be measured with the E-Perm radon monitor also known as an Electret Ion Chamber (EIC), which is a passive integrating ionization monitor. This system consists of the electret reader, chambers, and electrets. For measuring radon indoors, the electrets must be fixed into the chambers then placed inside the study area of homes. The difference between the voltages inside the electrets before the chamber is opened is measured. After the study time is finished, the voltage of the electrets is again measured. The difference between the first voltage reading & the second reading is the amount of discharge in the electrets. The amount of discharge is then used to calculate radon concentration indoors in  $\text{Bq/m}^3$ .

## **Part (3): Instrumentation and Set Up**

For this project, many instruments are used to measure the radioactivity concentrations of the study area. Collected samples (soil and water) were carried out using gamma ray spectrometry and ion conductivity plasma-mass spectrometer (ICP-MS). For this project, a field portable gamma-ray spectrometer (EnviSpec GR 320) is used that assays concentrations of potassium ( $^{40}\text{K}$ ), thorium ( $^{232}\text{Th}$ ) and uranium ( $^{238}\text{U}$ ) elements and total counts in the area of study. Radon in air and water are measured separately by E-PERM and RAD-7 devices respectively.

### **1) Gamma Ray Spectrometer:**

Gamma ray spectrometry was used for estimation of the activity concentration of potassium ( $^{40}\text{K}$ ), thorium ( $^{232}\text{Th}$ ) and uranium ( $^{238}\text{U}$ ) elements Bq/kg, in soil sample. The Gamma ray spectrometer, as shown in Figure 3-3, consists of:

- A hyper pure germanium coaxial detector (CANBARRA Model CR401950, N-type and 40 % relative efficiency) of a vertical configuration that is mounted on a 30 liter liquid nitrogen Dewar for germanium crystal temperature control. The preamplifier is coupled to the detector and connected to the germanium crystal, so that its input components are kept at liquid nitrogen temperature.
- High voltage power supply is designed to supply the detector with high voltage, with positive or negative polarity, with very low noise and very high voltage stability. All this is necessary to achieve the proper operation of a high resolution germanium detector.
- Bin and power supply (NIM standard) with  $\pm 6$ ,  $\pm 12$ ,  $\pm 24$  volt.
- Spectroscopy amplifier which is an integral part of the low noise system. In addition to providing high amplification gain, it provides shaping of the signal pulse in order to obtain the optimum signal to noise ratio consistent with the counting rate.
- Analog-to-digital converter (ADC) which is intended to offer the ultimate in resolution, stability and linearity.
- Multichannel Analyzer with 8192 channels and with counting capacity of  $2^{28}$  counts per channel.

### **Setting up:**

To reduce the gamma ray background, the hyper pure germanium detector is inserted inside a lead shield, through a hole in the bottom. The lead shield is internally lined with cadmium and copper layers. To reduce the noises from thermal radiation in the crystal, the HPGe detector is cooled with liquid nitrogen ( $77^\circ\text{K}$ ) during its use. This will reduce the leakage current generated by mobile carriers at room temperature and prevent voltage break down through the crystal. The HPGe gamma ray spectrometer was set up according to the arrangements shown in, Figure 3 and Figure 4.

The coarse and fine gain controls of the spectroscopy amplifier, the differentiating and integrating time constants and all other controls were adjusted. This afforded the best energy resolution and good linearity of the spectrometer over a wide band of the input voltages. After selecting the optimum set up, the resolving power of the spectrometer was found to be 1.92 KeV for 1332 KeV gamma ray line of the  $^{60}\text{Co}$ .

### **Calibration:**

The gamma ray spectrometer was calibrated applying different gamma emitters. These include cesium-137 (661.66 KeV), cobalt-60 (1173.23 KeV, 1332.5 KeV), potassium-40 (1460.8 KeV) and radium-226 with gamma ray lines shown in Table 1 [22]. Obviously, the radium-226 is most favorable for calibration, since its spectrum covers a wide energy range from 0.186 MeV to 2.45 MeV.

#### **(a) Energy calibration and peak identification:**

The energy calibration was done using three gamma ray lines with well-known energies of  $^{137}\text{Cs}$  and  $^{60}\text{Co}$  point sources. These energy values are fitted to a third order equation of the following form:

$$E = A_0 + A_1 X + A_2 X^2 + A_3 X^3$$

Where,  $E$  is the energy of the photo-peak in keV,

$X$  is the channel number, and

$A_0, A_1, A_2$  and  $A_3$  are fitting coefficients that are used to determine the energy of any unknown photo-peak.

**(b) Efficiency calibration of HPGe detector:**

Through two stages, the efficiency calibration in the energy range from 186 KeV to 2450 KeV was performed in two stages. In the 1<sup>st</sup> stage, the relative efficiency curve of the detector was obtained using a  $^{226}\text{Ra}$  point source. The most intensive gamma rays of  $^{226}\text{Ra}$  in equilibrium with its daughters have been used. The relative intensities of the photo-peaks corresponding to these gamma ray lines have been measured by the detector calculated. The photo-peak relative efficiency was obtained by dividing the relative intensity of the photo-peak with energy ( $E$ ) by the reference relative intensity of the same photo-peak, i.e.

$$\epsilon(E) = I_M(E) / I_R(E)$$

Where,  $\epsilon(E)$ : is the relative efficiency at energy ( $E$ ),

$I_M$  : is the relative intensity measured by the detector for the photo peak with Energy ( $E$ ), and

$I_R$  : is the reference relative intensity of the photo-peak at the same energy.

The relative efficiency curve of the detector was made of 17 different energy values covering the energy range from 186 keV to 2450 keV. The relative efficiency curve was obtained for two different positions. First, the source was placed in coaxial position at 15 cm distance from the top surface of the detector. Second, the source was put at the same distance from the detector in a lateral position. The efficiency curve was plotted for both source positions and it was found that the two curves within a good approximation coincide within the energy range between 240 keV and 2450 keV. A slight difference was found at energies range less than 240 keV. Using both results, an averaging curve, sixth order polynomial fitting was made as shown in Figure 5. The relative efficiency of the detector corresponding to any photo-peak energy can be then obtained using this averaged curve.

In the second stage, the average relative efficiency curve of the detector was normalized to an absolute efficiency. The normalization has been done using standard solutions of potassium chloride.

The gamma transitions used for activity calculations of  $^{40}\text{K}$  and  $^{137}\text{Cs}$  are 1460 keV and 661.6 keV respectively. Those for  $^{238}\text{U}$  series are 351.9 keV ( $^{214}\text{Pb}$ ), 609.3 keV ( $^{214}\text{Bi}$ ), 1120.3 keV ( $^{214}\text{Bi}$ ) and 1764.5 keV ( $^{214}\text{Bi}$ ). Those for  $^{232}\text{Th}$  series are 338.4 keV ( $^{228}\text{Ac}$ ), 583 keV ( $^{208}\text{Tl}$ ), 911.1 keV ( $^{228}\text{Ac}$ ), and 968.9 keV ( $^{228}\text{Ac}$ ). The gamma transitions, used for calculation of natural radionuclide concentrations, are shown in Figure 6. The calculated activity concentrations were corrected for the sample density.

**1. Inductively Coupled Plasma-Mass Spectrometry, ICP-MS:**

The water sample was analyzed at the Saudi geological survey laboratories (Jeddah) using Perkin Elmer Elan 9000 ICP-MS and Varian Radial Spectrometer ICP-AES.

**2. Field portable gamma-ray spectrometer EnviSpec GR 320 (Figure 7):**

For this project, field portable gamma-ray spectrometer EnviSpec GR 320 as shown in Figure 7 is used to give the concentration of natural occurring ground radioactive nuclides ( $^{238}\text{U}$ ,  $^{232}\text{Th}$  and  $^{40}\text{K}$ ) and total count. The GR-320 Environmental Gamma Ray Spectrometer analyzes the intensities and energies of all gamma rays to calculate total exposure or dose rate. An extensive library of nuclides and their respective energies is used for nuclide identification.

The standard system utilizes a high sensitivity 76x76 mm (3"x3") NaI crystal for monitoring environmental levels of both man-made and natural gamma radiation.

The system is calibrated to calculate and display the concentrations of potassium, uranium and thorium. For this, several measurement points have been set. These points are distributed randomly around the study area. Each point is separated from the others by distances of around 350m-550m to give a clearer view of the background radiation of the study area and to measure the effective annual dose. From GR 320 data, concentration maps of radioactive elements can be drawn.

**3. RAD7 Electronic Radon Monitor/Sniffer (Figure 8):**

RAD7 is a simple computer-driven electronic detector, with pre-programmed set-ups for common tasks, where radon is measured in pCi/L. This instrument has a built-in air pump, rechargeable batteries, and a Hewlett-Packard alpha-numeric graphics printer with infra-red link.

To make this device work, a purging process must be done through a gas drying unit containing  $\text{CaSO}_4$  gravels (Figure 9). After the purging process, a water bottle is connected to the device through special hoses (Figure 10).

#### **4. e-Perm system for Radon indoor measurement (Figure 11):**

An E-PERM, also known as an Electret Ion Chamber (EIC), is a passive integrating ionization monitor consisting of a very stable electret mounted inside a small chamber made of electrically conducting plastic. The electret, a charged Teflon® disk, serves as both the source for ion collection and as the integrating ion sensor. Negative ions produced inside the chamber are collected on the positively charged electret, causing a reduction of its surface charge.

The measurement of the depleted charge during the exposure period is a measure of integrated ionization during the measurement period. The electret charge is read before and after the exposure using a specially built non-contact electret voltage reader referred to as the SPER-1 Electret Voltage Reader. Using this data as input to the appropriate formula, one can determine the radon activity present over the duration of the test. The basic components of the E-PERM® System consist of the electret reader, chambers, and electrets. There are chambers of different sizes and electrets of different sensitivities to meet a wide range of monitoring situations. Typically, a more sensitive electret, referred to as an ST Electret, is used for short-term measurements, and an LT, or less sensitive electret, is used for longer term measurements. They are known as “true integrators” because they are constantly collecting and “registering” the ions generated by the radon decaying inside the chamber.

### **Part (4): Calculations**

#### **1- Detection Limits:**

The detection limit is the fundamental limitation of a particular measuring system to distinguish a net signal from a background signal with a predetermined level of confidence. This limit is established prior to and is dependent upon the intrinsic instrument background and any reagent blank activity introduced in the chemical separation procedure. The detection limit is independent of the sample size or concentration of a radionuclide in the original material. Detection limits indicate our ability to measure activity with a particular system. With this limitation known, it is possible to estimate the necessary sample size to detect activity with a stated degree of confidence.

In the development of a detection limit, the important factors are the instrument background, the reagent blank activity, the instrument detection efficiency, the chemical yield of the separated sample, and the duration of the measurement. The detection limit can be reduced by changes and improvements in these factors [14 and 23]. It can be represented by the following equation:

$$MDA = K \times 1.65 \sqrt{\frac{F}{(t_f)^2}} \left[ 1 + \frac{N_p}{N_f} \right]$$

Where, MDA is the minimum detectable activity,  
K is Bq/kg per counting rate,  
F is the background counts for the measuring time  $t_f$ ,  
 $N_p$  is the number of channels affected by the peak, and  
 $N_f$  is the number of channels used for assessing the background area.

#### **2- Analytical Quality Control:**

Quality control measurements are necessary to provide documentation to show that the achieved analytical results are reliable. The reliability of the results is a function of precision (reproducibility) and accuracy (true value). Analysis should be performed using many different methods & techniques as possible.

In addition, control analysis with reference materials that are as similar as possible to the materials to be analyzed is desirable. It is advisable on a routine basis to participate in inter-laboratory comparisons. Agreement between certified or most probable mean value and observed value is a direct measure of accuracy for the particular determination.

The status of equipment should be checked routinely by measuring background, blanks, and standards. These results often give the first indication of analytical difficulties. Analytical control samples generally constitute about 10-15 % of the total radioactivity samples [24]. The quality control measurements include periodic calibrations of counting instruments using traceable standards and routine measurement of instrument backgrounds.

#### **3- Dose Assessment:**

The absorbed dose rate (nGy/h), and dose equivalent rate (nSv/h) in air one meter above the ground level at each location were calculated using the following equation [25].

$$D = R_K C_K + R_U C_U + R_{Th} C_{Th}$$

Where,  $D$ : is the absorbed dose rate,

$R_K$ ,  $R_U$ , and  $R_{Th}$ : are the conversion factors, expressed in nGy/h per Bq/kg. These conversion factors are given in Table 3.

$C_K$ ,  $C_U$ , and  $C_{Th}$ : are the concentrations of  $^{40}K$ ,  $^{238}U$ , and  $^{232}Th$ , respectively, expressed in Bq/kg.

## **RESULTS AND DISCUSSIONS**

The elements of radiological assessment include the specific radionuclide's released, their transport, bioaccumulation, & uptake by humans, doses resulting from the uptakes, & an estimation of the risk due to the dose [26-28]. The process is illustrated in Figure 12. In most cases, radiological assessment is performed using models, because environmental data are obviously not available when predictions for the future are being made, because environmental data are frequently sparse or unavailable for historical studies.

For radionuclide release, the basic source term information is the kind and quantity of activity released per unit time. The chemical and physical properties of the release are also very important because transport and accumulation depend on these properties. The source may be moved by air or water, which then transport and disperse the radionuclides in the environment. Transport and dispersion by air, surface water, and ground water is complex but has been studied extensively. Transport models are developed based on the basic behavior of radionuclides in these media. As the radionuclides move through the atmosphere and hydrosphere they are absorbed (and eliminated) by plants and animals.

### **1- Measurements of Activity concentration of radionuclides in Soil Samples using Gamma-ray spectrometry:**

The  $^{238}U$ ,  $^{232}Th$  and  $^{40}K$  concentration in a soil sample was determined directly by using a shielded coaxial High Purity Germanium (HPGe) detector.

Based on the radioactivity levels of  $^{238}U$ ,  $^{232}Th$  and  $^{40}K$ , the gamma absorbed dose rate in air (ADRA) in nGy h<sup>-1</sup> at one meter above the ground level was calculated using the following formula [24]:

$$ADRA = 0.427 C_U + 0.667 C_{Th} + 0.043 C_K$$

Where:

ADRA : is the absorbed dose rate at 1 meter above ground (nGy h<sup>-1</sup>).

$C_U$ ,  $C_{Th}$  and  $C_K$ : are activity concentrations (Bq kg<sup>-1</sup>) of  $^{238}U$ ,  $^{232}Th$  and  $^{40}K$ , respectively, in soil sample.

The measured dose rates in air at one meter above the ground level from terrestrial gamma radiation is the annual effective dose (AED) in  $\mu$ Sv was calculated as follows:

$$AED = ADRA \times DCF \times OF \times T$$

Where:

ADRA : absorbed dose rate in air (nGy h<sup>-1</sup>).

DCF : dose conversion factor of 0.7  $\mu$ Sv Gy<sup>-1</sup>.

OF : is the outdoor occupancy factor of 0.2.

T : is the time (8760 h y<sup>-1</sup>).

A dose conversion factor (DCF) and outdoor occupancy factor (OF) were used as recommended by the UNSCEAR.

The activity concentrations of  $^{238}U$ ,  $^{232}Th$  and  $^{40}K$  in soil samples, calculated and measured gamma absorbed dose rate, and effective dose rate in air at 1 m above the ground are given in Table 4.

### **2- Activity concentration of radionuclides in Water Samples using Inductively Coupled Plasma - Mass Spectrometry, ICP-MS:**

Uranium is a naturally occurring long-lived radionuclide, which is known for both its radio-toxicity and chemical toxicity. In order to assess its effect to public health, knowledge is necessary about the distribution and transfer of U in the soil-water plant system, especially in agricultural fields. Uranium and other heavy metal impurities may accumulate in the soil [29] and be leached into ground and surface water where they can be taken up by plants and transferred into the food chain. Concentration of uranium (ppb) and other elements in underground water sample is given in Table 5. Generally, the occurrence of radionuclides in the underground water is mainly due to the leaching of the salts from the bed-rocks.

The concentration of uranium in water depends on several factors. These include the uranium concentration in the aquifer rock, the partial pressure of carbon dioxide, and the presence of oxygen and complexation agents in the aquifer. The characteristics of water that mainly determine its capacity to dissolve, carry or deposit elements are its pH, temperature, redox potential, concentration and properties of dissolved salts, flow rate, and residence time [30].

The health effects and risk of uranium can be divided into radiological risk of uranium isotopes and the

chemical risk as a toxic heavy metal. US Environmental Protection Agency (EPA) has classified uranium as a confirmed human carcinogen (group A). EPA has suggested that only zero tolerance is a safe acceptable limit for the carcinogenic risk from uranium and has finalized realistic regulation levels as maximum contaminant level (MCL) The "minimal risk" level for intermediate-duration ingestion proposed by the EPA [31] is an oral uptake of 2 µg of uranium per kg body weight/day.

The World Health Organization (WHO) has established a Tolerable Daily Intake (TDI) for uranium of 0.6 µg/kg body weight per day [WHO1998, WHO2003]. This is based on adverse effects observed by Gilman [1998a] with the kidneys of rats at uptakes of 60 µg U/kg/day. When uranium gets inside the body it can lead to cancer or kidney damage.

### **3- Activity concentration of radionuclides in soil samples using field Portable gamma-ray spectrometer EnviSpec GR 320:**

For this project, field portable gamma-ray spectrometer EnviSpec GR 320 is used to determine the amount of concentration of natural occurring ground radioactive nuclides ( $^{238}\text{U}$ ,  $^{232}\text{Th}$  and  $^{40}\text{K}$ ) and total count. The GR-320 Environmental Gamma Ray Spectrometer analyzes (see above comment-2TJR) the intensities and energies of all gamma rays to calculate total exposure or dose rate. An extensive library of nuclides and their respective energies is used for nuclide identification. Table 6 shows the results in field and Table 7 shows the results after calculations formula of Beck, HL (1972):

From the measured dose rates in air at one meter above the ground level from terrestrial gamma radiation; the annual effective dose (AED) in µSv was calculated. A geographic information system program called ArcGIS v 9.3 is used to draw concentration maps from the results to identify the high dose zones in the area shown in Figures 12, 13, 14, 15, 16 and 17. These 5 maps explain the results in an appropriate way. The red zones are the highest zones and the green zones are the lowest radiation dose. Observe that in Figure 17, the highest zones occurred in occupied regions which are the most dangerous.

### **4 Radon indoors and in water sample:**

#### **1 Radon Measurements in Water:**

Radon is a radioactive gas that emanates from rocks and soils and tends to concentrate in enclosed spaces like underground mines or houses. Soil gas infiltration is recognized as the most important source of residential radon. Other sources, including building materials and water extracted from wells, are of less importance in most circumstances. Radon is a major contributor to the ionizing radiation dose received by the general population.

Recent studies on indoor radon and lung cancer in Europe, North America and Asia provide strong evidence that radon causes a substantial number of lung cancers in the general population. Current estimates of the proportion of lung cancers attributable to radon range from 3 to 14%, depending on the average radon concentration in the country concerned and the calculation methods.

The analyses indicate that the lung cancer risk increases proportionally with increasing radon exposure. As many people are exposed to low and moderate radon concentrations, the majority of lung cancers related to radon are caused by these exposure levels rather than by higher concentrations. Radon is the second cause of lung cancer after smoking. Most of the radon-induced lung cancer cases occur among smokers due to a strong combined effect of smoking and radon.

Radon measurements are relatively simple to perform and are essential to assess radon concentration in homes. They need to be based on standardized protocols to ensure accurate and consistent measurements. Indoor radon concentration varies with the construction of buildings and ventilation habits. These concentrations not only vary substantially with the season but also from day to day and even from hour to hour. Because of these fluctuations, estimating the annual average concentration of radon in indoor air requires reliable measurements of mean radon concentrations for at least three months and preferably longer.

Short-term measurements provide only a crude indication of the actual radon concentration. Quality assurance for radon measurement devices is highly recommended in order to ensure the quality of measurements. Addressing radon is important both in construction of new buildings (prevention) and in existing buildings (mitigation or remediation). The primary radon prevention and mitigation strategies focus on sealing radon entry routes and on reversing the air pressure differences between the indoor occupied space and the outdoor soil through different soil depressurization techniques. In many cases, a combination of strategies provides the highest reduction of radon concentrations.

The choice of radon prevention and mitigation interventions can be based on an analysis of cost-effectiveness. In this approach, net health-care costs are set in relation to net health benefits for a variety of actions or policies, providing an index with which these actions can be prioritized.

Selected analyses indicate that preventive measures in all new buildings are cost effective in areas where more than 5% of current dwellings have radon concentrations above 200 Bq/m<sup>3</sup>. Prevention in new homes tends to be more cost-effective than mitigation of existing homes. In some low-risk areas the measurement costs

may be higher than the mitigation costs (for existing dwellings) due to the high number of homes that will have to be tested compared to the proportion of homes mitigated. Even if analyses indicate that remediation programs are not cost-effective on a nationwide basis, indoor radon at high concentrations poses a considerable risk of lung cancer for individuals and requires mitigation.

Since the general public is often unaware of the risks associated with indoor radon, special risk communication is recommended. Radon risk communication needs to be focused on informing the different audiences and recommending appropriate action on reducing indoor radon. A cooperative effort is required, involving technical and communication experts, to develop a set of core messages.

Radon risk messages should be kept as simple as possible and quantitative risk information must be expressed to the public in clearly understandable terms. It is useful, for example, to place the risk of lung cancer due to radon in comparison with other cancer risks, or with common risks in everyday life.

Public health programs to reduce the radon risk should be ideally developed on national level. Such national radon programs would be designed to reduce the overall population's risk from the national average radon concentration as well as the individual risk for people living with high radon concentrations.

A national radon policy should focus on identifying geographical areas where populations are most at risk from radon exposures and raising public awareness about the associated health risk. Key elements for a successful national program include collaboration with other health promotion programs (e.g. indoor air quality, tobacco control) and training of building professionals and other stakeholders involved in the implementation of radon prevention and mitigation. Appropriate building codes that require the installation of radon prevention measures in homes under construction should be enacted, and the measurement of radon during the purchase and sale of homes is useful to identify those with high radon concentrations.

A national reference level for radon represents the maximum accepted radon concentration in a residential dwelling and is an important component of national programs. For homes with radon concentrations above these levels remedial actions may be recommended or required. When setting a reference level, various national factors such as the distribution of radon, the number of existing homes with high radon concentrations, and the arithmetic mean indoor radon level and the prevalence of smoking should be taken into consideration. In view of the latest scientific data, WHO proposes a reference level of 100 Bq/m<sup>3</sup> to minimize health hazards due to indoor radon exposure.

However, if this level cannot be reached under the prevailing country-specific conditions, the chosen reference level should not exceed 300 Bq/m<sup>3</sup> according to recent calculations by the International Commission on Radiation Protection [WHO handbook on indoor radon, Hajo Zeeb, 2009].

Radiation dose rate and health risk for an individual exposed to a known concentration of radon and its decay products over 70 years is calculated using World Information Service on Energy (WISE) web site calculator [<http://www.wise-uranium.org/epusaf.html>]. The concentration of radon indoors is plotted for a better view as shown in Figure 18.

## **2 Radon Measurements in Water:**

The <sup>222</sup>Rn concentration in water is due to the decay of <sup>226</sup>Ra associated with the rock and soil. Apparently, the radon gas percolates through the soil and rock, and dissolves in the water. Therefore, the concentration of radon in water is higher than one would expect if the activity were due only to supporting dissolved <sup>226</sup>Ra in the water. Even so, since radon is the immediate daughter of <sup>226</sup>Ra, radon measurements have significance for determining the amount of <sup>226</sup>Ra in water as well. To date, no maximum permissible concentration levels (MCL's) exist for radon in drinking water although radon is expected to join radium (<sup>226</sup>Ra and <sup>228</sup>Ra) on the U.S. EPA list of regulated radionuclides. The maximum concentration level (MCL) for radon is expected to be relatively low (300 pCi L<sup>-1</sup>). The U.S. Environmental Protection Agency (EPA) estimates that a person has a 1 percent (1 in 100) risk of developing cancer from life-long household use and consumption of water containing 20,000 pCi/L of dissolved radon.

Using RAD7 device for well water samples from the study area gives a reading of 817 pCi/L radon concentration in the water sample. The cancer risk of this concentration is calculated and it is 3% (1:70) percent of risk of developing cancer from life-long household use and consumption of water containing 817 pCi/L of dissolved radon.

## **SUMMARY AND CONCLUSIONS**

People are exposed to a variety of environmental agents, including biologic, chemical, and physical entities, in the air they breathe, the water they drink, the food they eat, the surfaces they contact, and the products they use. Sometimes exposures to environmental toxicants are sufficient to cause adverse health consequences such as birth defects, cancer, neurobehavioral effects, and respiratory disease. The quantitative estimation of such health risks based on information about exposure and dose-response relationships is fundamental to policy decisions about which risks are unacceptable and how best to manage them. There is a great interest in the study of natural environmental radiation in soil and rocks because the population is exposed to this radioactivity at different levels depending on those radioactive minerals in each region in the world.

Naturally occurring radiation and environmental radioactivity has led to extensive surveys in many countries of the world. Radioactivity surveys have been used since the late 1940's in the exploration for uranium and uranium bearing rocks. Natural environmental radioactivity arises mainly from primordial radionuclides, such as  $^{40}\text{K}$  and the nuclides from the  $^{232}\text{Th}$  and  $^{238}\text{U}$  series and their decay products, which occur at trace levels in all ground formations. Primordial radionuclides are formed by the process of nucleo-synthesis in stars and are characterized by half-lives comparable to the age of the earth. Natural environmental radioactivity and the associated external exposure due to gamma radiation depend primarily on the geological and geographical conditions, and appear at different levels in the soils of each region in the world. The specific levels of terrestrial environmental radiation are related to the composition of each litho-logically separated area, and to the content of the rock from which the soils originate.

Researchers reported an increase of some natural radionuclides and heavy metals in the Arabian shield region soil and rocks. Due to the high elevation of this region, the cosmic radiation dose will also increase.

Thirty one soil samples and one water sample were collected from thirty two locations in agricultural and residential region in Taif called wadi Muhrim. Activity concentration of  $^{238}\text{U}$ ,  $^{232}\text{Th}$ ,  $^{40}\text{K}$  and  $^{222}\text{Rn}$  were measured using a well calibrated gamma-ray spectrometry system based on hyper pure germanium detector (HPGe). Leachable and total concentration of uranium, in the water sample using inductively coupled plasma-mass spectrometry (ICP-MS). In addition, a GR 320 field portable gamma-ray spectrometer EnviSpec was used in the field to measure  $^{238}\text{U}$ ,  $^{232}\text{Th}$ ,  $^{40}\text{K}$  concentrations in the soil. Indoor radon concentrations were also measured in 10 houses and the cancer risk for individuals was calculated. The cancer risk from radon in the water well sample was calculated from measurements using RAD7 instrument.

The average activity concentrations of  $^{238}\text{U}$ ,  $^{232}\text{Th}$ ,  $^{40}\text{K}$  and  $^{222}\text{Rn}$  are within the world average. The annual effective dose is seriously affected by altitude due to cosmic radiation. Uranium concentration in the water sample was found to be more than the World Health Organization (WHO) has established for a Tolerable Daily Intake (TDI) of uranium (0.6  $\mu\text{g}/\text{kg}$  body weight per day) [32].

It will be very useful to perform the same study in other areas in the kingdom with similar geology pattern in order to have a complement and complete conclusion for the findings in our study.

The final conclusion is

1. The average effective dose rates are within the average national and world recommended values.
2. It is highly recommended for people in old houses to use modern techniques to reduce the amount of radon gas concentrations.
3. It is also recommended that those who are living in the high potential radioactive areas to move to lower locations.

As a recommendation for further future work we suggest the following:

- It is important to conduct further studies on the vertical distributions of the natural radionuclides on soil.
- It is recommended to expand this study for the whole wadi Muhrim region to give a complete view of terrestrial radiation assessment of this region and to produce mapping for radioactivity concentration in the entire Wadi Muhrim.

## REFERENCES

- 1- White, R.E. 1987; "Introduction to the Principles and practices of soil science"; Black well Pub.
- 2- Merdanoglu B., Altinsoy N., 2006; Radioactivity concentrations and dose assessment for soil samples from Kestanbol granote area; Radiation protection and dosimetry 121 (4), 399-405.
- 3- UNSCEAR, 1993. "Sources Effects and Risks of Ionizing Radiation United Nations Scientific Committee on the effects of Atomic Radiation", Report to the general Assembly, with annexes. United Nations, New York.
- 4- UNSCEAR, 2000. "Sources Effects and Risks of Ionizing Radiation United Nations Scientific Committee on the effects of Atomic Radiation", Report to the general Assembly, with annexes. U N, NY.
- 5- Radhakrishna, A.P., Somashekarappa, H.M., Narayana, Y., Siddappa, K., 1996. Distribution of some natural & artificial radionuclides in Mangalore environment of South India. J. Environ. Radioact. 30, 31-54.
- 6- Quindo's, L.S., Ferna'ndez, P.L., Soto, J., Ro' denas, C., Go' mez, J., 1994. Natural radioactivity in Spanish soils. Health phys 66, 194-200 .
- 7- El-Reefy .H.I, Sharshar .T, Zaghoul .R, Badran .H.M.,2006, "Distribution of gamma-ray emitting radionuclides in the environment of Burullus Lake: I. Soils and vegetations, J. of Environmental Radioactivity 87,148-169.
- 8- NRC 2011 Nuclear Regulatory Commission (U.S.), "Fact Sheet on Biological Effects of Radiation" (2004, available at: <http://www.nrc.gov/reading-rm/doc-collections/fact-sheets/bio-effects-radiation.html>, January 2011

- 9- Abdul-Majid, S., Abulfaraj, W., 1992. Radioactivity concentration in soil in Jeddah area, Saudi Arabia; J. Environ. Sci. Health A27, 105e116
- 10- Al Hamarneh, I., Wreikat, A., Toukan, K., 2003. Radioactivity concentrations of  $^{40}\text{K}$ ,  $^{134}\text{Cs}$ ,  $^{137}\text{Cs}$ ,  $^{90}\text{Sr}$ ,  $^{241}\text{Am}$ ,  $^{238}\text{Pu}$  &  $^{23}\text{Pu}$  &  $^{240}\text{Pu}$  radionuclides in Jordanian soil samples. J. Environ. Radioact. 67, 53-67.
- 11- Tawfik A. Al Kuasayer and A. Abdulla Nowman Al Haj, 1987, "Measurement of the natural radiation background level of Riyadh city", Transaction of American Society 55(2), pp. 87-89.
- 12- Bazilevskaya, G.A., Usoskin, I.G., Flückiger, E.O., Harrison, R.G., Desorgher, L., Büttikofer, R., Krainev, M.B., Makhmutov, V.S., Stozhkov, Y.I., Svirzhevskaya, A.K., Svirzhevsky, N.S. and Kovaltsov, G.A., 2008, "Cosmic Ray Induced Ion Production in the Atmosphere", *Space Sci. Rev.*, **137**, 149–173
- 13- International Atomic Energy Agency (IAEA) ,1979. Gamma-ray surveys in uranium exploration. Technical Report Series No. 186, International Atomic Energy Agency
- 14- Commission of the European Communities, 1993. "Radiation protection; Fifth international symposium on the natural radiation environment", Report EUR, 14411 EN.
- 15- UNSCEAR, 1988. "Sources Effects and Risks of Ionizing Radiation United Nations Scientific Committee on the effects of Atomic Radiation", Report to the general Assembly, with annexes. United Nations, New York.
- 16- Eisenbud, M., 1987, "Environmental Radioactivity From Natural, Industrial and Military Sources" Academic Press, Inc.
- 17- Oosterhuis, L., 1992 "Radiological Aspects of the Non-Nuclear Industry in the Netherlands" Radiation Protection Dosimetry, Vol. 45, No. (1-4), pp. 703-705.
- 18- Abrahams P.W., 2002. Soils: their implications to human health. The Science of the Total Environment 291, 1–32
- 19- Blanco Rodriuez, P., Vera Tome, F., Lozano, J.C., Perez-Fernandez, M.A., 2008, "Influence of soil texture on the distribution and availability of  $^{238}\text{U}$ ,  $^{230}\text{Th}$  and  $^{226}\text{Ra}$  in soils", Environmental Radioactivity 99, 1247-1254.
- 20- Leung, K.C., Lau, S.Y., Poon, C.B., 1990. Gamma radiation dose from radionuclides in Hong Kong soil. J. Environ. Radioact. 11, 279-290
- 21- International Center for Agricultural Research in the Dry Areas (ICARDA), "The standard procedures according to ICARDA organization", Aleppo, Syria, [[www.icarda.org/publications/lab\\_manual/read.htm](http://www.icarda.org/publications/lab_manual/read.htm)].
- 22- Farouk, M. A., Souraya, A. M., 1982. Ra-226 as standard source for efficiency calibration of Ge(Li) detector. Nuclear Instruments and Methods 200, 593-595.
- 23- IAEA , 1989, "Measurement of radionuclides in food & the environment" Technical report series No. 295.
- 24- Beck H.L., Decampo J., and Gogolok C. "Insitu Ge(Li) and NaI(Tl) gamma ray spectrometry" HASL - 258, Health and Safety Laboratory, U.S. Atomic Energy Commission, New York, 1972.
- 25- Beretka, J., Mathew, P.J., 1985, Natural radioactivity of Australian building materials, industrial wastes and by-products, Health Physics 48, 87–95.
- 26- National Council on Radiation Protection and Measurement, 1975. "Natural Background Radiation in the United States" NCRP report No. 45.
- 27- National Council on Radiation Protection & Measurement, 1984. "Radiological Assessment: Predicting the Transport, Bioaccumulation, & uptake by Man of Radionuclide Released to the Environment" NCRP Report. No.76.
- 28- National Council on Radiation Protection and Measurements, 1992 "Exposure of the Population in the United States and Canada from Natural Background Radiation" NCRP Report No. 94.
- 29- Rothbaum, H.P., McGaveston, D.A., Wall, T., Johnston, A.E., Mattingly, G.E.G., 1979, "Uranium applications in soils from long-continued applications of super- phosphate", J. Soil Science 30, 147-53.
- 30- Shabana E, Al-Hobaib A, 1999. "Activity concentrations of natural radium, thorium and uranium isotopes in ground water of two different regions", Radiochim, Acta 87, 41-54
- 31- ATSDR/EPA Community Meeting In Corina, Maine, 1999, "Priority List for Top 20 Hazardous Substances".
- 32- WHO handbook on indoor radon: a public health perspective/edited by Hajo Zeeb, & Ferid Shannoun, 2009.

Table 1: Summary of the activity concentration of  $^{238}\text{U}$  ( $^{226}\text{Ra}$ ),  $^{232}\text{Th}$  ( $^{228}\text{Ra}$ ) and  $^{40}\text{K}$  (Bq/kg) in soil samples worldwide [El-Reefy et al., 2006]

Location	$^{238}\text{U}$ (or $^{226}\text{Ra}$ )	$^{232}\text{Th}$ (or $^{228}\text{Ra}$ )	$^{40}\text{K}$	Note	Ref
<b>Africa</b>					
Algeria	5-27	7-27	93-412	Sand	Noureddine et al., 1997
Egypt	3-101	2-117	16-1379	National range	El-Reefy et al., 2006
Libya	8.7-12.8	7.6-9.7	265-282	Tripoli	Shenber, 1997
Namibia	45-49	3-38	42-1,100		Steinhausler and Lettner, 1992
<b>Asia</b>					
Bangladesh	37.2 (15-94)	60 (28-129)	438 (200-772)	Coastal	Chowdhury et al., 1999
China	18.2-79.7	2.33-225	281-891		Ziqiang et al., 1988
Hong Kong	30-110	1.9-243	59-851		Leung et al., 1990
India	20-62	14-48	61-317	Coastal	Narayana et al., 2001
India	16 (5-71)	119 (15-776)	406 (200-854)	Kalpakkam	Kannan et al., 2002
India	11.1 <sup>b</sup> (3.1-15.9)	8.9 (3.8-16.9)	108	Mangalore Soil	Radhakrishna et al, 1996
India	3.6 <sup>b</sup> (2.8-4.9)	5.6 (4.8-6.2)		sand	
Jordan			156-544		Al Hamarneh et al., 2003
Kuwait	11.8(1.8-28)	10(1.5-16)	332(4-497)		Bou-Rabee, 1997
Oman	29.7	16	225		goddard, 2002
Saudi Arabia	9.3	7.4	369	Jeddah area	Abdul-Majid and Abulfaraj, 1992
Syria	22.2 (1-40)	18.4 (11-25)	247 (100-378)		Othman and Yassine, 1995
Taiwan	11-33	14-44	148-814		Pao-Shan, 1996
<b>Europe</b>					
Canary Island	7.3-104	12-111	142-1489		Fernande-Aldecoa et al., 1992
Greece	21-80	16-85	337-1380		Florou and Kritidis, 1992
Greece	7-310	3-190	30-1440	All provinces	Probonas and Kritidis, 1993
Greece	25 (1-238)	21 (1-193)	355 (12-1570)		Anagnostakis et al., 1996
Ireland		3-60	40-800		Mcaulay and Morgan 1988
Italy	57-71	73-87	580-760		Bellia et al, 1997
Norway	43.3 (12-137)	21.1 (4-52)	283 (31-564)	Costal	Dowdall et al ,2003
Serbia	21-29	25-43	348-441		Djuric et al, 1996
Spain	13-165	7-204	48-1586		Baeza et al ,1992
Spain	38.3 (36.2-40.5)	41 (38.9-43.7)	653 (617-689)	Caceres Province	Baeza et al ,1994
Spain	8-310	5-258	31-2040	National survey	Quindos et al, 1994
Spain	20-711	13-84	289-703		Martinez-Aguirre and Garcia leon, 1997
<b>Americas</b>					
Brazil	29.2 (10-137)	47.8 (12-191)	704 (56-1972)	Rio Grande do Norte	Malanca et al, 1996
Brazil	2.7-21	3.5-24	12-435	South Shetland Islands	Godoy et al, 1998
Canada	15.6 (3.3-36)	12.3 (1.5-28)	416 (153-817)	Northem Ontario	Vande nbygaart and Protz, 1999
Costa Rica	10	8	175	Rainforest	Bossey and Strelb, 2001
USA	41	82	930	New Jersey	Shebell and Miler, 1996
Venezuela			44-886		Labrecuque et all, 1992
Global average	25 (10-50)	25 (7-50)	370 (100-700)		UNSEAR , 1988

Table 2: Relative intensities of gamma-rays from  $^{226}\text{Ra}$  with its short-lived gamma emitting daughters ( $^{214}\text{Pb}$  and  $^{214}\text{Bi}$ ) [Farouk, Souraya, 1982].

No.	Isotope	Gamma-ray energy (KeV)	Relative intensities		
1	<b>Ra-226</b>	<b>186.18</b>	<b>9.07</b>	$\pm$	<b>0.14</b>
2	<b>Pb-214</b>	<b>241.92</b>	<b>16.53</b>	$\pm$	<b>0.31</b>
3	Pb-214	258.82	1.72	$\pm$	0.04
4	<b>Pb-214</b>	<b>295.22</b>	<b>42.52</b>	$\pm$	<b>0.59</b>
5	<b>Pb-214</b>	<b>351.99</b>	<b>81.29</b>	$\pm$	<b>0.81</b>
6	Pb-214	545.77	0.63	$\pm$	0.02
7	Bi-214	480.50	0.68	$\pm$	0.02
8	Pb-214	487.25	0.83	$\pm$	0.03
9	<b>Bi-214</b>	<b>609.31</b>	<b>100.00</b>	$\pm$	
10	Bi-214	665.45	2.87	$\pm$	0.06
11	Bi-214	703.11	0.82	$\pm$	0.03
12	<b>Bi-214</b>	<b>768.36</b>	<b>10.64</b>	$\pm$	<b>0.03</b>
13	Bi-214	806.17	2.49	$\pm$	0.60
14	Bi-214	839.20	1.30	$\pm$	0.03
15	<b>Pb-214</b>	<b>934.06</b>	<b>6.54</b>	$\pm$	<b>0.13</b>
16	Bi-214	1051.96	0.76	$\pm$	0.03
17	<b>Bi-214</b>	<b>1120.29</b>	<b>33.52</b>	$\pm$	<b>0.42</b>
18	Bi-214	1155.19	3.65	$\pm$	0.07
19	<b>Bi-214</b>	<b>1238.11</b>	<b>13.25</b>	$\pm$	<b>0.22</b>
20	Bi-214	1280.96	3.22	$\pm$	0.06
21	<b>Bi-214</b>	<b>1377.67</b>	<b>8.66</b>	$\pm$	<b>0.16</b>
22	<b>Bi-214</b>	<b>1509.23</b>	<b>4.77</b>	$\pm$	<b>0.09</b>
23	Bi-214	1583.22	1.57	$\pm$	0.03
24	Bi-214	1666.28	2.55	$\pm$	0.05
25	<b>Bi-214</b>	<b>1729.60</b>	<b>6.56</b>	$\pm$	<b>0.12</b>
26	<b>Bi-214</b>	<b>1764.50</b>	<b>34.91</b>	$\pm$	<b>0.41</b>
27	<b>Bi-214</b>	<b>1847.42</b>	<b>4.59</b>	$\pm$	<b>0.09</b>
28	<b>Bi-214</b>	<b>2118.50</b>	<b>2.51</b>	$\pm$	<b>0.05</b>
29	<b>Bi-214</b>	<b>2204.21</b>	<b>10.66</b>	$\pm$	<b>0.20</b>
30	Bi-214	2293.36	0.67	$\pm$	0.02
31	<b>Bi-214</b>	<b>2447.81</b>	<b>3.28</b>	$\pm$	<b>0.06</b>
32	Bi-214	2694.82	0.08	$\pm$	0.00
33	Bi-214	2770.02	0.05	$\pm$	0.00
34	Bi-214	2978.80	0.02	$\pm$	0.00

Table 3: Conversion factors, expressed in nGy/h per Bq/kg [Beretka and Mathew, 1985].

The gamma energy lines used for relative efficiency calibration are bold.

Absorbed Dose rate (nGy/h)/(Bq kg <sup>-1</sup> )	Isotopes
0.043	<sup>40</sup> K
0.427	<sup>238</sup> U
0.662	<sup>232</sup> Th

Table 4 Radioactivity concentration of <sup>232</sup>Th, <sup>238</sup>U and <sup>40</sup>K in Wadi Muhrim soil sample, absorbed dose rate and effective dose rate in air from <sup>232</sup>Th, <sup>238</sup>U and <sup>40</sup>K.

Annual effective dose Rate (μSv)	Absorbed Dose Rate(nGy h <sup>-1</sup> )	t=28800 sec			Sample Name
		K-40	U-238	Th-232	
(Terrestrial)	(Terrestrial)	<b>(Bq/Kg)</b>			
25.75	21	359.51 ± 18.96	7.86 ± 2.80	2.94 ± 1.72	<b>WMR-02</b>
		111.72	47.8	45.77	<b>Standard</b>
		116.28	42.61	40.93	

Table 5: Uranium and other elements concentrations, and activity concentration of <sup>238</sup>U in water sample:

3	2	1	WHO	GCC & SASO STANDARDS	EPA	Elements		Seq. No
WMR-W1	WMR-W1	WMR-W1						
mBq/L	µgm/kg	ppb	ppb	ppb	ppb			
		1.47				Li	Lithium	1
		<0.50		1	4	Be	Beryllium	2
		292.34	500P	500		B	Boron	3
		2.34	200	200		Al	Aluminum	4
		0.22	500P	500		Mn	Manganese	5
		1.59	20P	20		Ni	Nickel	6
		0.98	2000P	2000	1300	Cu	Copper	7
		0.46	3000	3000		Zn	Zinc	8
		0.88	10P	10	10	As	Arsenic	9
		525.82				Br	Bromine	10
		0.10				Rb	Rubidium	11
		808.86				Sr	Strontium	12
		<0.10	U	100	5	Ag	Silver	13
		<0.10	3	3		Cd	Cadmium	14
		0.14	U	1		Sn	Tin	15
		<0.50	5	5	6	Sb	Antimony	16
		65.00				I	Iodine	17
		<0.10				Cs	Cesium	18
		77.73	700	700	2000	Ba	Barium	19
		<0.10				Ta	Tantalum	20
		<0.10	1	1	2	Hg	Mercury	21
		<0.10			2	Tl	Thallium	22
		0.10	10	10	15	Pb	Lead	23
		0.10				Bi	Bismuth	24
<b>19.8</b>	<b>1.52</b>	<b>1.52</b>	<b>2P</b>	<b>2</b>	<b>30</b>	<b>U</b>	<b>Uranium</b>	<b>25</b>
		0.31	50P	50	100	Cr	Chromium	26
		0.52	10	10	50	Se	Selenium	27

. This amount of uranium in water leads to: If the person ingested 500L/year the effective dose will be 0.93 µSv/year.

Table 6:  $^{238}\text{U}$ ,  $^{232}\text{Th}$  and  $^{40}\text{K}$  concentrations field results:

$^{232}\text{Th}$ ppm	$^{238}\text{U}$ ppm	k40%	T.C. ppm	Elev. (m)	Sam. No.
4.2	0.9	2.1	12.2	1846	WAD - 1
1.3	0.1	0.9	5.1	1859	WAD - 2
3.3	0.8	2.1	11.9	1845	WAD - 3
2.6	0.1	1.4	7.9	1842	WAD - 4
3.8	0.9	1.7	10.3	1833	WAD - 5
4.1	0.6	3	15.6	1844	WAD - 6
2.9	0.6	2.4	12.1	1845	WAD - 7
2.9	0.1	1.9	9.8	1838	WAD - 8
1.4	0	1.8	8.4	1859	WAD - 9
2.5	0.1	2.1	10.4	1844	WAD - 10
1.4	0.1	1.3	6.9	1845	WAD - 11
1.2	0	1.1	5.9	1839	WAD - 12
4	0.3	1.8	10.4	1844	WAD - 13
2.2	0.4	1.6	8.7	1839	WAD - 14
3.9	0.5	1.9	10.7	1838	WAD - 15
3.1	0.2	2.7	13.5	1856	WAD - 16
1.5	0	1	5.9	1843	WAD - 17
3.7	0	1.2	6.1	1850	WAD - 18
2.4	0.7	1.6	9.2	1848	WAD - 19
5	0.8	1.2	8.8	1845	WAD - 20
3.1	0.7	1.3	8.4	1847	WAD - 21
3	0.5	1.8	10.2	1846	WAD - 22
3.1	0.5	1.3	8.5	1840	WAD - 23
2.7	0.3	2.1	10.4	1841	WAD - 24
1.8	0	1	6	1840	WAD - 25
1.4	0.2	1.5	7.4	1852	WAD - 26
4.5	0.6	1.9	11.2	1840	WAD - 27
0.8	0	1.6	7.7	1851	WAD - 28
2.5	0.3	1.5	8.8	1844	WAD - 29
3	0.6	1.9	10.1	1857	WAD - 30

Table 7:  $^{238}\text{U}$ ,  $^{232}\text{Th}$ ,  $^{40}\text{K}$  and cosmic doses after calculations results:

Tot. mSv/a	TR. mSv/a	CR. mSv/a	Tot. nGy/h	$^{232}\text{Th}$ nGy/h	$^{238}\text{U}$ nGy/h	$\text{K}_{40}$ nGy/h	Th Bq/kg	U Bq/kg	$\text{K}_{40}$ Bq/kg	Cos. nSv/h	Elev. (m)	Sam. No.
0.92	0.26	0.65	43	10	5	27	17	11	657	75	1846	WAD - 1
0.75	0.10	0.66	16	3	1	12	5	1	282	75	1859	WAD - 2
0.90	0.25	0.65	40	8	5	27	13	10	657	75	1845	WAD - 3
0.81	0.15	0.65	25	6	1	18	11	1	438	75	1842	WAD - 4
0.88	0.22	0.65	37	9	5	22	15	11	532	74	1833	WAD - 5
0.98	0.32	0.65	53	10	3	39	17	7	939	75	1844	WAD - 6
0.91	0.26	0.65	42	7	3	31	12	7	751	75	1845	WAD - 7
0.85	0.20	0.65	32	7	1	25	12	1	595	74	1838	WAD - 8
0.82	0.17	0.66	27	3	0	23	6	0	563	75	1859	WAD - 9
0.86	0.21	0.65	34	6	1	27	10	1	657	75	1844	WAD - 10
0.78	0.13	0.65	21	3	1	17	6	1	407	75	1845	WAD - 11
0.76	0.11	0.65	17	3	0	14	5	0	344	74	1839	WAD - 12
0.87	0.21	0.65	35	10	2	23	16	4	563	75	1844	WAD - 13
0.83	0.18	0.65	29	5	2	21	9	5	501	74	1839	WAD - 14
0.88	0.23	0.65	37	10	3	25	16	6	595	74	1838	WAD - 15
0.93	0.27	0.66	44	8	1	35	13	2	845	75	1856	WAD - 16
0.76	0.10	0.65	17	4	0	13	6	0	313	75	1843	WAD - 17
0.81	0.15	0.66	25	9	0	16	15	0	376	75	1850	WAD - 18
0.84	0.19	0.65	31	6	4	21	10	9	501	75	1848	WAD - 19
0.85	0.20	0.65	32	12	5	16	20	10	376	75	1845	WAD - 20
0.83	0.18	0.65	29	8	4	17	13	9	407	75	1847	WAD - 21
0.86	0.21	0.65	34	7	3	23	12	6	563	75	1846	WAD - 22
0.82	0.17	0.65	27	8	3	17	13	6	407	74	1840	WAD - 23
0.87	0.22	0.65	36	7	2	27	11	4	657	74	1841	WAD - 24
0.76	0.11	0.65	17	4	0	13	7	0	313	74	1840	WAD - 25
0.80	0.15	0.66	24	3	1	20	6	2	470	75	1852	WAD - 26
0.89	0.24	0.65	39	11	3	25	18	7	595	74	1840	WAD - 27
0.80	0.14	0.66	23	2	0	21	3	0	501	75	1851	WAD - 28
0.82	0.17	0.65	27	6	2	20	10	4	470	75	1844	WAD - 29
0.88	0.22	0.66	36	7	3	25	12	7	595	75	1857	WAD - 30

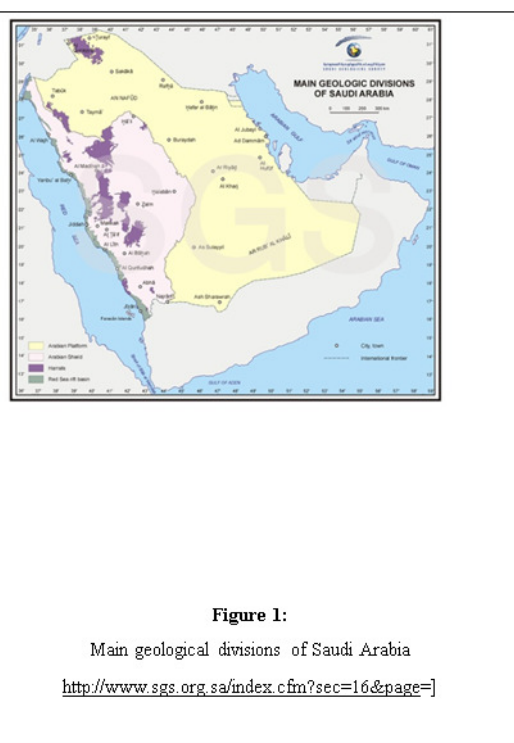
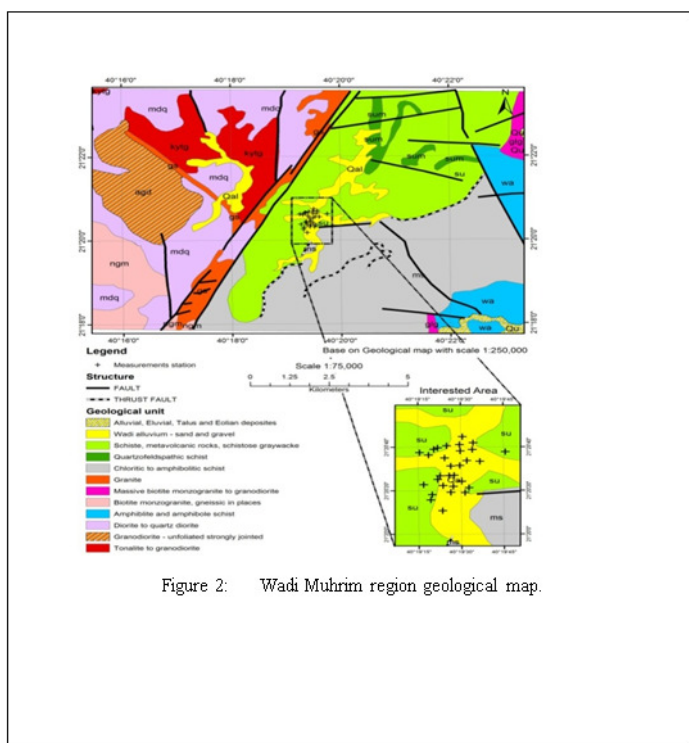
Due to the average annual effective dose for this region the cancer risk will be calculated over 70 years for public and a risk factor of 0.05 per Sv. The cancer risk will be 0.294% (1:340).

Table 8 summarizes the annual worldwide and the recommended effective doses [IAEA2001].

Wadi Muhrim Results (annual effective dose (mSv/a))	Typical effective dose range (mSv/a)	Worldwide average annual effective dose (mSv/a)	Source
0.65	0.3	0.4	<b>External Exposure:</b> <b>Cosmic rays</b> <b>Terrestrial gamma rays</b>
0.32	0.3	0.5	
<b>0.97</b>	<b>0.6</b>	<b>0.9</b>	

Table 9 shows the measured radon in the houses of the study area and the cancer risk of each measurement.

Excess lifetime cancer risk. (%)	Annual dose rate (mSv/a)	Concentration (pCi/L)	Concentration (Bq/M <sup>3</sup> )	V2 (volts)	V1 (volts)	Sample #
1.426% (1 : 70.13)	1.629	2.5	84.0	692	696	1
0.684% (1 : 146.1)	0.782	1.2	40.8	641	643	2
1.426% (1 : 70.13)	1.629	2.5	84.0	713	717	3
1.141% (1 : 87.66)	1.303	2.0	62.4	674	677	4
1.141% (1 : 87.66)	1.303	2.0	62.4	706	709	5
2.852% (1 : 35.06)	3.259	5.0	171.2	700	708	6
0.684% (1 : 146.1)	0.782	1.2	40.8	676	678	7
1.141% (1 : 87.66)	1.303	2.0	62.4	635	638	8
0%	0.00	0.0	0.0	715	715	9
9.697% (1 : 10.31)	11.08	17.0	630.3	689	718	10



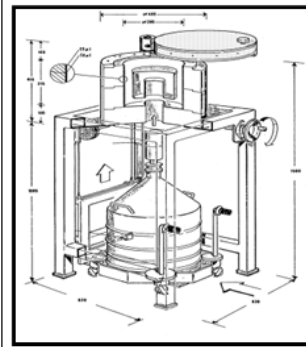


**Figure 4:** The arrangement of the HPGe detector with the lead shield [Farouk, Souraya, 1982].

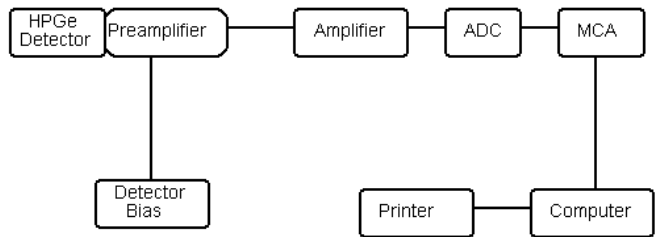


**Figure 3:** Block diagram of Gamma ray Spectrometer set up

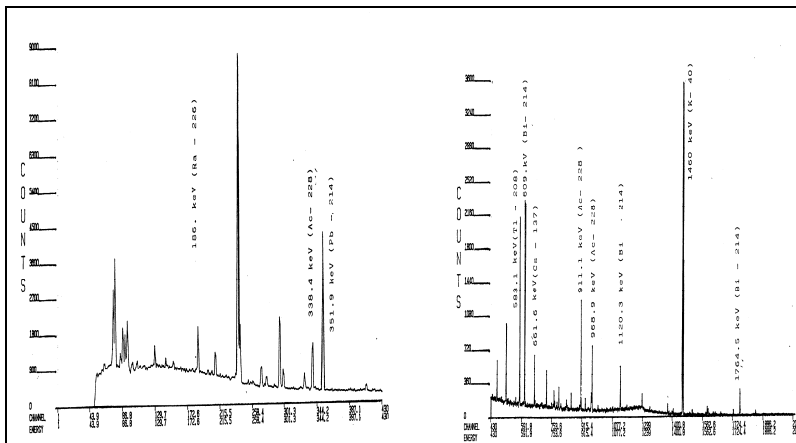


**Fig 6:** Gamma Transitions of <sup>238</sup>U Series, <sup>232</sup>Th Series, <sup>40</sup>K and <sup>137</sup>Cs [Farouk, Souraya, 1982].

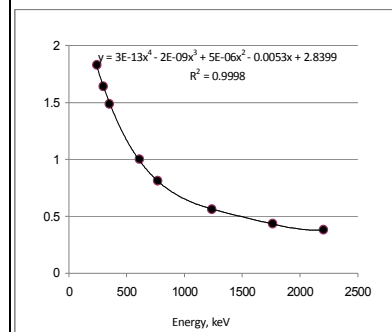


**Figure 5:** Relative efficiency of <sup>226</sup>Ra and its daughter's gamma energy lines.



**Figure 8** RAD7 Electronic Radon Monitor/Sniffer



**Figure 7** Field portable gamma-ray spectrometer EnviSpec GR 320



**Figure10:** RAD7 purgation process



**Figure11:** e-Perm Radon Indoor measurement system



**Figure 9** RAD7 gas drying unit

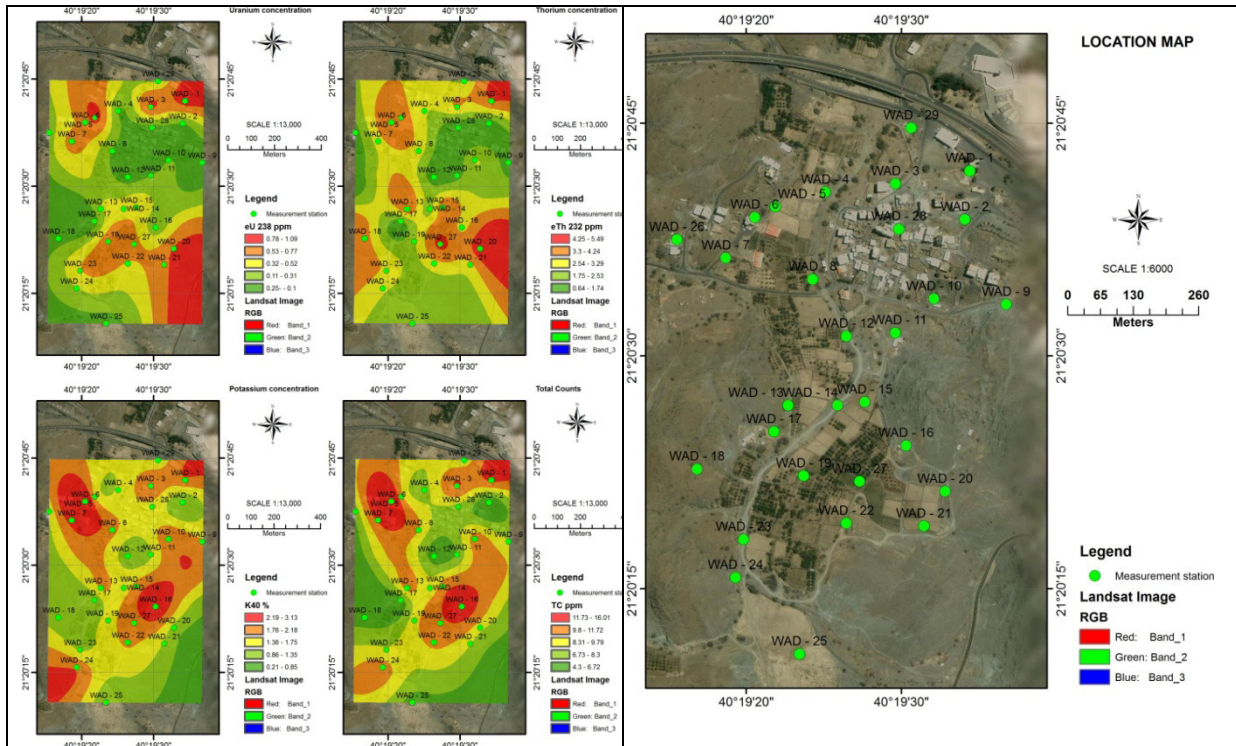


Figure 13: Shows the concentrations of Uranium, Thorium, Potassium and total count in the study area.

Figure 12: Shows the measurements stations in the study area.

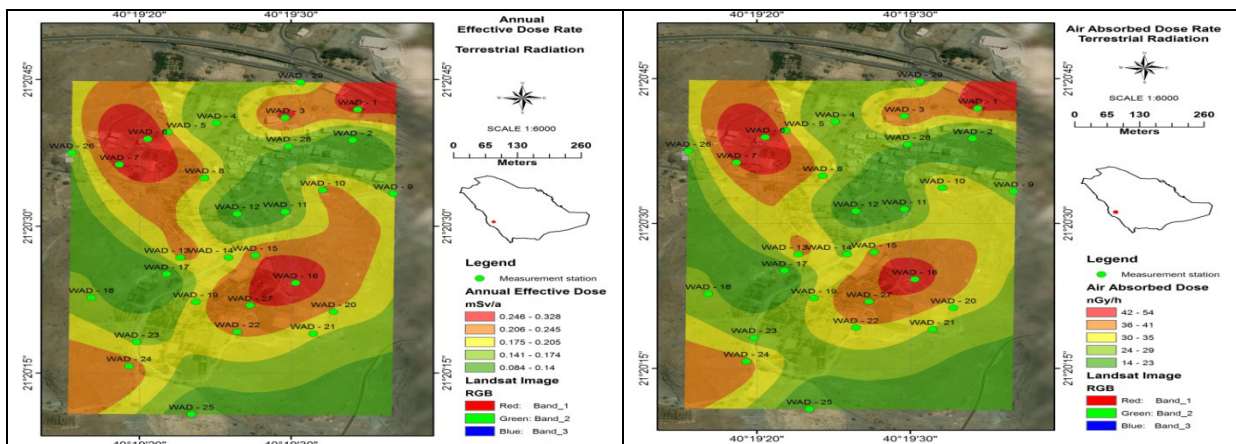


Figure 15: Shows the Annual Effective Dose rate from Terrestrial Radiation elements in the study area.

Figure 14: Shows the Air Absorbed Dose Rate of terrestrial elements in the study area.

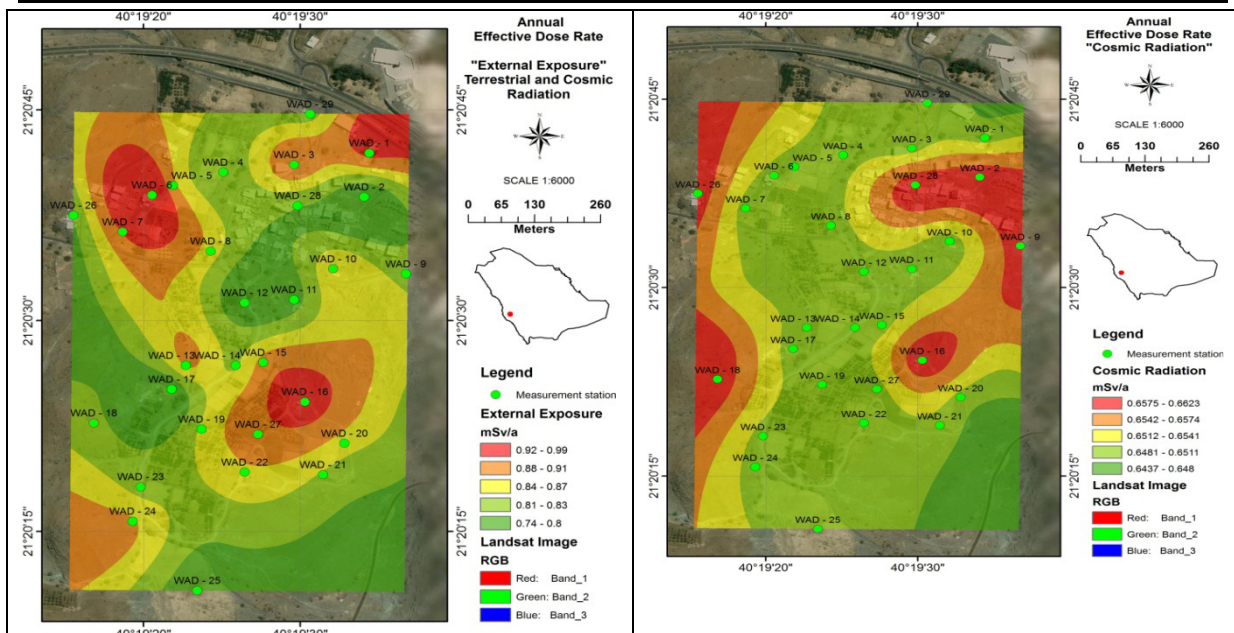


Figure 17: Shows the Annual Effective Dose rate from external exposure cosmic Radiation and terrestrial elements in the study area.

Figure 16: Shows the Annual Effective Dose rate from cosmic Radiation in the study area.

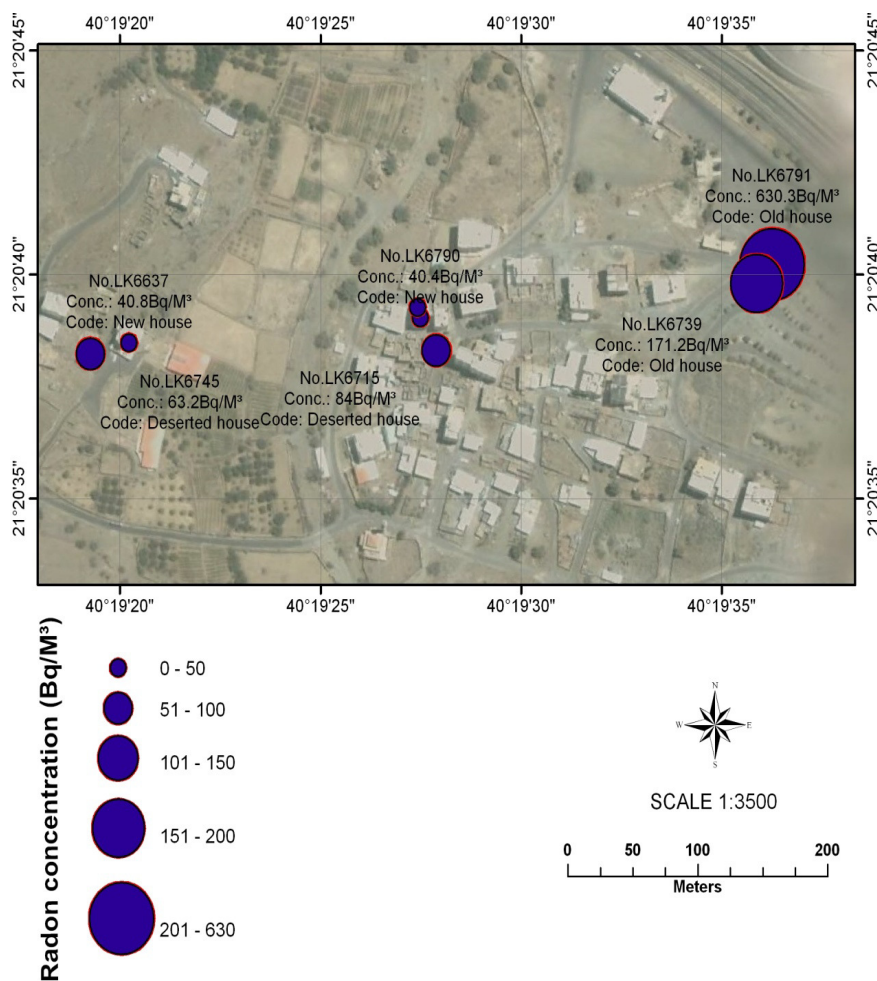


Figure 18: Shows the radon concentration indoors around the study area.

This academic article was published by The International Institute for Science, Technology and Education (IISTE). The IISTE is a pioneer in the Open Access Publishing service based in the U.S. and Europe. The aim of the institute is Accelerating Global Knowledge Sharing.

More information about the publisher can be found in the IISTE's homepage:

<http://www.iiste.org>

## CALL FOR PAPERS

The IISTE is currently hosting more than 30 peer-reviewed academic journals and collaborating with academic institutions around the world. There's no deadline for submission. **Prospective authors of IISTE journals can find the submission instruction on the following page:** <http://www.iiste.org/Journals/>

The IISTE editorial team promises to review and publish all the qualified submissions in a **fast** manner. All the journals articles are available online to the readers all over the world without financial, legal, or technical barriers other than those inseparable from gaining access to the internet itself. Printed version of the journals is also available upon request from readers and authors.

### IISTE Knowledge Sharing Partners

EBSCO, Index Copernicus, Ulrich's Periodicals Directory, JournalTOCS, PKP Open Archives Harvester, Bielefeld Academic Search Engine, Elektronische Zeitschriftenbibliothek EZB, Open J-Gate, OCLC WorldCat, Universe Digital Library, NewJour, Google Scholar

